OPEN ACCESS

GAVIN PUBLISHERS

Nanomedicine and Nanoscience Research

Research Article

Sendi R. J Nanomed Nanosci: JNAN-151.

DOI: 10.29011/2577-1477.100051

Structural and Electrical Behaviours of ZnO Nanoparticle-V_2O_5-Mn_2O_3 Varistor before and after Thermal Annealing in Different Atmospheres

Rabab Sendi*

Department of Physics, Faculty of Applied Science, Umm Al- Qura University (UQU), Makkah Al- Mukarramah, Saudi Arabia

***Corresponding author:** Rabab Sendi, Department of Physics, Faculty of Applied Science, Umm Al- Qura University (UQU), 21955 Makkah Al- Mukarramah, Saudi Arabia. Tel: +966565883532; Email: rksendi@uqu.edu.sa

Citation: Sendi R (2018) Structural and Electrical Behaviours of ZnO Nanoparticle-V_2O_5-Mn_2O_3 Varistor before and after Thermal Annealing in Different Atmospheres. J Nanomed Nanosci: JNAN-151. DOI: 10.29011/2577-1477.100051

Received Date: 04 August, 2018; **Accepted Date:** 20 August, 2018; **Published Date:** 27 August, 2018

Abstract

ZnO-based varistors are semiconductor ceramics whose excellent electrical behaviors are induced from their grain boundaries and dependent on their microstructural characteristics. In theory, fine primary particles with narrow size distributions provide enhanced structural and electrical properties. Thus, these properties are related to the morphological characteristics and size of ZnO grains. Most commercial ZnO varistors fabricated from microparticle-sized ZnO powder and composed of Bi_2O_3 exhibit excellent properties, but they have some drawbacks because of high sintering temperatures and high Bi_2O_3 volatility and reactivity. In this study, V_2O_5 is added to a varistor fabricated from 20 nm ZnO powder to reduce the sintering temperature, but the additive of V_2O_5 has no improvement in its electrical behaviors, and other additives are needed to obtain high performance. For this purpose, the nonlinear properties of this varistor can be enhanced by incorporating some oxide additives, such as Mn_2O_3, which are used as minor oxide additives. The effect of thermal annealing on the structural and electrical properties of the varistor is also investigated. A strong solid-state reaction during sintering may be attributed to the high surface area of 20 nm ZnO nanoparticles that promote a strong surface reaction. Results indicate that the non-ohmic behavior of varistors physically originates from oxygen on grain surfaces adsorbed by intrinsic defects. The electrical resistivity of the varistor is effectively minimized by thermal annealing in a reducing atmosphere, such as N_2 and N_2+10%H_2, possibly because the passivation of zinc ions and grain boundaries by hydrogen atoms increases mobility and carrier concentration. However, thermal treatment at lower than 400˚C is less efficient than that at other temperatures. The lowest resistivity is obtained during annealing at 200˚C in a N_2+10%H_2 atmosphere and 9.2 Ω/sq sheet resistance, which further increases as annealing temperature increases.

Keywords: Electrical Properties; Microstructure; Thermal Annealing; Varistor; Zno Nanoparticles

Introduction

With an excellent nonlinear coefficient and a low leakage current, varistor devices have been used in electronic and electrical systems, such as surge protection devices. The breakdown voltage and resistance of these varistors rely on microstructural conditions; as such, grain size and microstructural homogeneity are the most important parameters in varistor manufacturing [1]. One way to achieve these objectives is to use homogeneous ZnO nanoparticle powder for varistor fabrication. ZnO nano-scale particles have various chemical and physical properties compared with those of bulk materials. High homogeneity, enhanced sintering ability, and other unusual properties may be predicted because of large surface areas, nano-sized crystallites, and various surface properties [2]. Thus, the fabrication of varistors with ZnO nanoparticle powder should improve their properties tremendously. ZnO varistors are divided into Bi_2O_3- [3] and Pr_6O_{11}-based [4] varistors. However, V_2O_5 is added as a varistor-forming oxide that decreases the sintering temperature of varistors [5,6]. However, the addition of V_2O_5 does not improve electrical properties, and other oxide additives are necessary to obtain high performance; that is, the nonlinear characteristics of varistors can be enhanced by incorporating some oxide additives, which are used as minor oxide additives, such as MnO_X oxides (MnO, MnO_2, and Mn_2O_3) [6,7] and CoO_X oxides (CoO and Co_3O_4) [8]. The addition of different CoO_x oxides and MnO_x oxides in ZnO varistors helps detect different electrical characteristics, and the valence of the added oxides affects the nonlinear characteristics of ZnO ceramics.

To improve the crystalline quality of ZnO, we can implement thermal annealing treatment, which is a widely known effective technique. Annealing temperature plays an important role in controlling intrinsic defects in ZnO and properties of samples. At high annealing temperatures, samples can recrystallize, and the concentration of defects changes as annealing temperature and atmosphere are altered. Other important annealing parameters include ambient gas, time, and gas flow rate. Annealing is an important tool to modify the properties of varistors at high temperatures, extended exposures, and various atmospheres [9-12]. Wide-bandgap semiconductors, such as ZnO and SnO_2, tend to be sensitive to ambient atmosphere [13]. Their electrical characteristics, which are controlled by intrinsic electronic defect formation, can be considerably modified by exposure to a specific gas [14]. This influence, which depends on the surface-to-volume ratio of a material, is enhanced when a metal oxide is deposited in the form of a thin layer. In this work, thermal annealing under different conditions is used for ZnO nanoparticle-V_2O_5-Mn_2O_3varistors. The effect of heat treatments on the structural and electrical behaviors of varistor ceramics was also investigated.

Experimental Details

Sample Preparation

ZnO nanoparticle-V_2O_5-Mn_2O_3varistors were prepared via the conventional ceramic processing method involving ball milling, drying, pressing, and sintering. Oxide precursors of 99.9% purity were used. The composition consists of 99 mol% 20-nm ZnO+ 0.5 mol% V_2O_5 + 0.5 mol% Mn_2O_3 powder. The powder was blended with Poly Vinyl Alcohol (PVA) by mixing with distilled water in a ball milling jar for 6 hours. The ZnO slurry was dried at 60˚C in air for 1 hour and then was granulated by sieving through a 20-mesh sieve. The resulting granules were used to make discs by pressing at 4 ton/cm^2 pressure. The green ZnO discs were 26 mm in diameter and 2 mm thick. Finally, the green discs were sintered at 900˚C in air for 1 h. The as-grown ZnO varistors were annealed in O_2, N_2 and N_2+10%H_2, respectively, and the temperature was varied from 200 to 800˚C.In order to measure the electrical properties, silver pastes were coated and toasted on both sides of the sintered samples.

Characterization

The crystalline phases were studied using a high resolution X-Ray Diffractometer (XRD) equipment (PANalytical X' Pert PRO MED PW3040) with Cu K_α radiation (ʎ=1.5406Å). Surface roughness was determined and surface images were taken by atomic force microscopy (AFM model BURKER).

Electrical Testing

The I - V characteristics of the samples were measured using a high voltage source measure unit (KEITHLEY instruments 246 high voltage supply). Impedance measurements were taken using a frequency response analyzer (HP 4294A) at frequencies ranging from 40 Hz to 15 MHz, with an amplitude voltage of 0.5 V. The carrier concentration, carrier mobility and electrical resistivity of the were determined by Hall effect measurement (HEM-2000). Sheet resistance was performed in this work by using a Sheet Resistance/Resistivity Measurement system, model: Changmin Tech CMT-SR2000N.

Results and Discussion

Microstructural Analysis

Figure 1 shows the X-Ray Diffraction (XRD) spectra of the ZnO-V_2O_5-Mn_2O_3varistors made from ZnO nanoparticle powder and annealed in O_2, N_2, and N_2+10%H_2 at 700˚C. The varistor samples were characterized by the strongest major peaks of (101), (100), (002), and (110), which were from the ZnO layer and emphasized through the polycrystalline nature of the varistors. Other peaks, such as $(Zn_3(VO_4)_2)$ and (Mn_3O_4) phases, are secondary phases, and ZnO varistors are multiphase materials. ZnO varistor materials contain ZnO as a major phase. Spinal, pyrochlore, and several other phases are present in the specimen. The presence of these phases is dependent on their processing parameters and the amount and nature of oxide additives to ZnO. The incorporation of these oxide additives forms atomic defects at the ZnO grain and grain boundary; donor or donor-like defects dominate the depletion layer, and acceptor and acceptor-like defects dominate the grain boundary states [15].

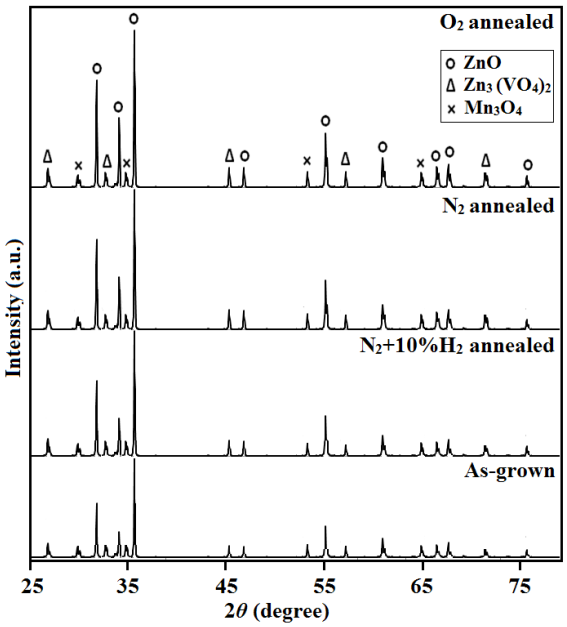

Figure 1: The X-ray diffraction patterns of the as grown ZnO nanoparticles-V_2O_5-Mn_2O_3varistorsat room temperature and annealed in O_2, N_2, N_2+10%H_2 at 700˚C.

Although several peaks of the disc annealed in an oxygen atmosphere are slightly higher than those of the discs annealed in other environments, the diffraction peaks of all of the samples are higher and narrower than those of the as-grown varistor sample, and the FWHM of the former during annealing is smaller than that of the later. This result indicates that the crystallinity and structural ordering of ZnO in the grain and grain boundaries are enhanced, and the sample annealed in O_2 atmosphere is of high quality. The XRD pattern (101) major peak corresponds to a peak shift of 0.15˚ toward a higher diffraction angle for the samples annealed in N_2 and to a peak shift of 0.16˚ for the samples annealed in N_2+10%H_2 compared with that of the as-grown sample possibly because of the chemisorption of N_2 or H_2 on the surface of the varistor after annealing, resulting in the distortion of crystallites [16,17]. ZnO nanoparticles exhibit a thermodynamically stable crystallographic phase, and the intensity of the peaks reflects a high degree of crystallinity. However, the width of the peaks increases because of the effect of quantum size on ZnO nanoparticles.

During annealing in an O_2 atmosphere, oxygen vacancies are complemented dominantly by chemisorption, and they combine with sufficient Zn atoms to produce new ZnO, thereby leading to an increase in XRD peaks during annealing in an O_2 atmosphere. However, annealing in a N_2 ambient can easily lead to perversion from the stoichiometric state, forming a significant oxygen deficiency. Oxygen complemented via annealing in an O_2 atmosphere reduces the amount of oxygen defects, suggesting that the structure and stoichiometry of the ZnO varistor annealed in an O_2 atmosphere are better than those annealed in N_2 or N_2+10%H_2 environments. The crystal size of the varistors was calculated using Scherrer's formula [18,19]:

$$D = 0.9\,\lambda / \beta\,\mathrm{Cos}\theta$$

Where λ = 1.54 Å, β= (B2 − b2) 1/2, B is the observed FWHM, and b is the instrument function determined from the broadening of the monocrystalline zinc diffraction line. The (101) diffraction peak is considered to calculate the crystal size. The crystal sizes are nearly the same as those of the varistors before and after they are annealed in O_2 or N_2+10%H_2. However, the crystal size of the samples annealed in N_2 slightly increases. The increase in the size of the grain can be attributed to the generation of oxygen vacancies in a N_2 atmosphere as vacancy concentration exponentially increases with an increase in temperature. This atmosphere may affect the kinetics of grain growth by changing the diffusion flux of oxygen vacancy types.

The 3D AFM images of the ZnO-V_2O_5-Mn_2O_3varistors annealed in different atmospheres at various annealing temperatures reveal rough and non-uniform structures. The surface roughness of the structure of the varistor annealed in O_2 is lower than that of the structure in other atmospheres. The Root Mean Square (RMS) roughness of the varistors annealed in diverse atmospheres is improved (Figure 2) with the variation of annealing temperatures. The RMS roughness of the varistors annealed in an O_2 atmosphere at 200˚C decreases slightly. As the annealing temperatures further increase, the roughness increases. The surface roughness and morphological characteristics can affect carrier mobility [20]. Surface roughness can be attributed to the increased grain size and secondary growth during annealing. Lin et al. [21] reported that high temperatures can stimulate the migration of grain boundaries and thus result in the coalescence of more grains during annealing. Fang et al. [22] further indicated that high activation energy should be available for atoms at high temperatures so that they may diffuse and occupy the correct site in a crystal lattice. Consequently, grains with low surface energies grow and enlarge. Grain growth also contributes to the increased surface roughness and enlarged microcracks [23,24].

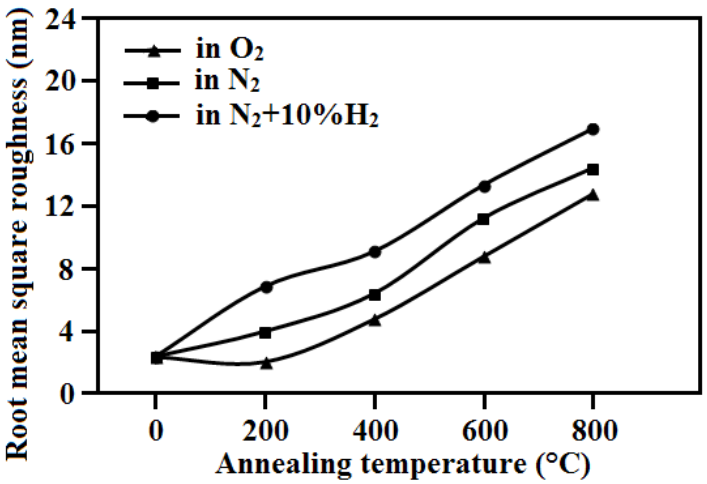

Figure 2: The Root Mean Square roughness (RMS) of the as grown ZnO nanoparticles-V_2O_5-Mn_2O_3varistors annealed under different atmosphere with the variation of annealing temperatures.

Thermal annealing at different temperatures significantly affect the surface roughness of the varistors fabricated from the ZnO nanoparticle powder because of the large surface-to-volume ratio of nanoparticles, thereby promoting oxygen or nitrogen absorption during annealing and forming an increased grain size.

Electrical Properties

The V-I curves of the as-grown ZnO nanoparticle-V_2O_5-Mn_2O_3 varistors and annealed in different annealing environments are plotted in Figure 3. Some electrical parameters, such as E_b and α, are listed in Table 1. These results show that the breakdown voltage reduces when ZnO nanoparticles are used to fabricate the varistors. The reduction in breakdown voltage can be clarified by the increase in the average grain size after sintering is completed, thereby reducing the number of grain boundaries between electrodes and decreasing "P-N Junctions". Decreased "P-N Junctions"

result in reduced breakdown voltages. The grain size within the varistor sample increases noticeably after sintering because of the significant surface area of ZnO nanoparticles. The addition of Mn_2O_3 to ZnO promotes grain growth and allows ZnO grains to enlarge, thereby reducing the breakdown voltage in the varistor. The V-I nonlinear behavior of the ZnO disc is a phenomenon of the grain boundaries between semiconducting ZnO grains. The breakdown voltage of the varistors is directly proportional to the number of grain boundaries per unit of thickness and inversely proportional to the size of ZnO grain. Decreased "P-N Junctions" result in reduced breakdown voltages. The grain size within the varistor sample increases noticeably after sintering because of the significant surface area of ZnO nanoparticles. The addition of Mn_2O_3 to ZnO promotes grain growth and allows ZnO grains to enlarge, thereby reducing the breakdown voltage in the varistor. The V-I nonlinear behavior of the ZnO disc is a phenomenon of the grain boundaries between semiconducting ZnO grains. The breakdown voltage of the varistors is directly proportional to the number of grain boundaries per unit of thickness and inversely proportional to the size of ZnO grain.

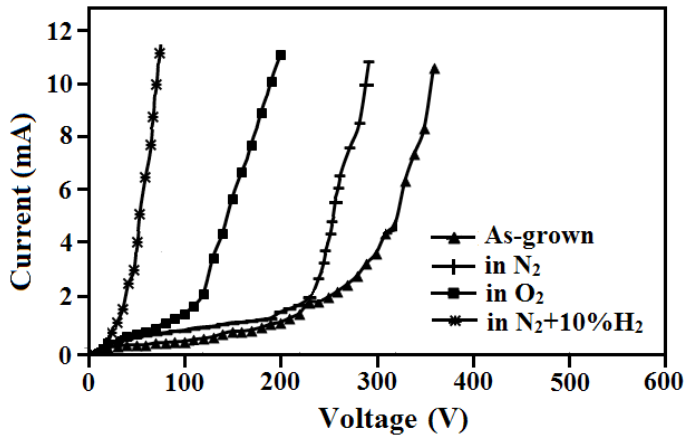

Figure 3: Current-Voltage characteristic of the as grown ZnO nanoparticles-V_2O_5-Mn_2O_3varistorsat room temperature and annealed in O_2, N_2, N_2+10%H_2 at 700°C.

Annealing atmosphere	E_b (V)	α	N_d(m^3) (x10^{20})	N_{IS}(m^{-2}) (x10^{12})	Φ_B (eV)	ω (nm)
As-grown	282	43	59.3	40.7	0.30	9.5
O_2	118	74	74.8	60.6	0.87	11.7
N_2	238	55	54.8	49.5	0.24	4.8
N_2+10%H_2	22	8	37.1	19.8	0.48	6.1

Table 1: Some electrical characteristic parameters of ZnO nanoparticles-V_2O_5-Mn_2O_3varistors annealed under different atmosphere at various temperatures.

The as-grown sample is nonlinear with a nonlinear coefficient α of 43, which is consistent with the value reported by Makarov et al. [25]. Its nonlinearity disappears after it is subjected to heat treatment in N_2+10%H_2 atmosphere. However, the nonlinear properties appear again by repeating the thermal treatment in O_2 atmospheres. The influence of atmospheric treatment at 700°C on E_b and α is significant (Table 1). Annealing in N_2 atmosphere decreases the nonlinear properties of the varistors. However, thermal annealing in the O_2 atmosphere significantly improves the non-ohmic value. The different behaviors of varistors in various annealing atmospheres are attributed to the potential barrier formation and to the O_2 species at the ZnO grain boundary that causes a Schottky-like barrier and trapping states. This improvement in the nonlinear properties of these varistors is associated with the degree of oxidation (when a varistor is annealed in an O_2 atmosphere) or reduction (when a varistor is annealed in an N_2 atmosphere) of metal oxide additives precipitated at the ZnO grain boundary. Sonderet al. [26] fabricated traditional ZnO-based varistors from ZnO microparticle powder and obtained similar results regarding these varistors annealed in oxidizing and reducing atmospheres. Santos et al. [27] reported that electrical behaviors are strongly affected by the atmosphere because of the oxidizing mechanism at the ZnO grain boundary. Bueno et al. [28] showed that thermal annealing in N_2 atmosphere decreases the surface states (N_{IS}) of a double (back-to-back) Schottky barrier and potential barrier height values.

However, thermal annealing in an O_2 atmosphere results in a considerable increase in (N_d) and (N_{IS}) states in a thin region of the grain boundary. Many approaches have suggested that thermal annealing fundamentally changes the electronic states of the grain boundary region [29]. Thus, the physical origin of the interfacial states is an extrinsic effect obtained from metal atoms precipitated at ZnO grain boundaries, not an intrinsic effect caused by a lattice mismatch at grain boundaries [29,30]. Electrical characteristics, such as nonlinear coefficient and barrier voltage, increase, and breakdown voltage decreases when the varistors are annealed in an O_2 atmosphere (Table 1). These results confirm that the electrical behaviors of the varistors are logical for oxygen species that exist on the grain boundary. Thermal annealing treatment in O_2 atmosphere is used in manufacturing, thereby prolonging the life of varistors. Another result is the re-establishment of the electrical behavior of the degraded varistors because of the adsorption of oxygen species at grain boundaries after these varistors are annealed in O_2 atmosphere. Oxygen in the grain boundary region is essential for the property of various varistor ceramics.

Impedance spectroscopy is an efficient technique to characterize grain boundaries in varistor ceramics [31]. In our study, complex impedance plots are derived from the as-grown sample and the sample annealed in the O_2 atmosphere Figure 4(a), displaying a grain-boundary semicircle. This finding indicates that grain boundaries are highly resistive regions. The spectra obtained from the varistors treated in N_2 and N_2+10%H_2 atmospheres Figure 4(b) are devoid of any grain boundary semicircle. Therefore, resistive grain boundary layers disappear, and the grain interior

is the only contribution to the frequency response of the varistors. However, the spectral shape implies the existence of inductive impacts, which are similar among various varistor samples [32]. The resistance of grain boundary is completely recovered after varistors are thermally annealed in O_2 atmosphere. Thus, the adsorption of O_2 in grain boundaries, which produce a resistive surface layer, is the origin of the electrical properties of the ZnO nanoparticle-V_2O_5-Mn_2O_3varistors. Santos et al. [33] revealed that atmosphere strongly influences the electrical properties because of the oxidizing mechanism at the grain boundary.

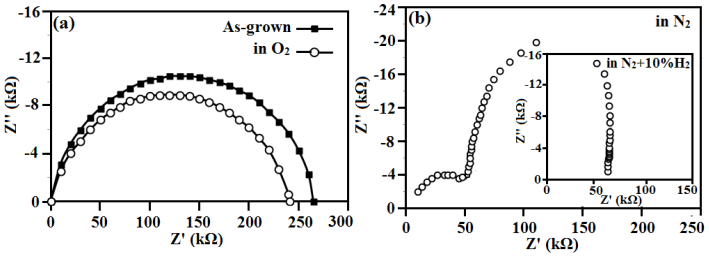

Figures 4(a,b): Complex impedance plots of the as grown ZnO nanoparticles-V_2O_5-Mn_2O_3 varistors at room temperature and annealed in various atmosphere at 700˚C.

The electrical resistivity, the carrier concentration, and the mobility of ZnO nanoparticle-V_2O_5-Mn_2O_3varistors annealed in different atmospheres as a function of annealing temperature are shown in Figure 5. The electrical resistivity of ZnO nanoparticle-V_2O_5-Mn_2O_3varistors is significantly reduced by annealing in N_2+10%H_2 atmosphere (Figure 5). Furthermore, annealing in a N_2 atmosphere decreases resistivity, although it is not as effective as thermal annealing in N_2+10%H_2. However, resistivity increases as annealing temperature increases from 200˚C to 800˚C in N_2+10%H_2 and from 400˚C to 800˚C in N_2. Resistivity is increased by annealing in an O_2 atmosphere. Doped ZnO varistors present the characteristics of n-type semiconductors because of the existence of zinc interstitials, oxygen vacancies, and hydrogen impurities, whereas Mn-doped varistors exhibit strong n-type conductor or semiconductor characteristics. Resistivity also increases rapidly as annealing temperature increases in the case of O_2 annealing possibly because zinc interstitial and oxygen vacancy concentrations decrease as expressed in the following reactions [34]:

$$Zn_{Zn} + V_o + ½\ O_2 \rightarrow ZnO \qquad (1)$$

$$Zn_i + ½\ O_2 \rightarrow ZnO \qquad (2)$$

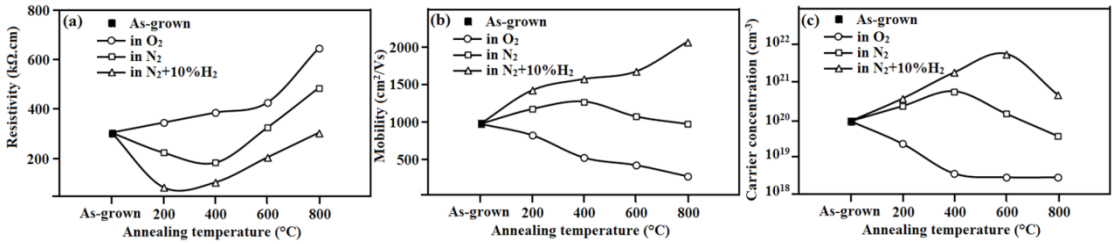

Figure 5: Electrical properties of the ZnO nanoparticles-V_2O_5-Mn_2O_3 varistors as function of annealing temperature in different atmospheres.

Reducing zinc interstitial and oxygen vacancy concentrations leads to a decrease in mobility and carrier concentrations because they act as donors and lead to ionized impurity scattering or impurity scattering [34]. As annealing temperature increases, reactions (1) and (2) accelerate remarkably.

In the case of N_2 or N_2+10%H_2 annealing, resistivity initially decreases and subsequently increases as thermal annealing temperature increases possibly because of the desorption of negatively charged oxygen species from the grain boundary region, which acts as a trapping site during annealing and forms potential barriers [35]. Negatively charged species create depletion regions near grain boundaries, thereby reducing mobility and carrier concentration. Hydrogen atoms passivate the surface of the grain boundary during annealing in a N_2+10%H_2 atmosphere, and this passivation of hydrogen atoms leads to the removal of depleted regions near grain boundaries. Thus, the removal of these region causes an increase in mobility and carrier concentration [36]. As well as the effect of the boundary passivation of hydrogen atoms, hydrogen impurity atoms also passivate Zn grain ions, which also contribute to an increase in carrier concentrations [36]. Crystallinity is improved by annealing in O_2 as revealed by XRD analysis (Figure 1), and this improvement may contribute to the increase in mobility and carrier concentration, but this contribution appears negligible because the mobility and carrier concentration of the varistors annealed in an O_2 atmosphere tend to reduce as the annealing temperature increases from 200˚C to 800˚C (Figure 5).

Table 2 presents the sheet resistance of ZnO nanoparticle-V_2O_5-Mn_2O_3varistors annealed in different atmospheres at various annealing temperatures. The as-grown sample yields a sheet resistance of 12 Ω/sq. However, the sheet resistance initially decreases as the annealing temperature increases to 400˚C in a N_2 and N_2+10%H_2 atmosphere. As annealing temperature exceeds 400˚C, the sheet resistance increases significantly. The initial decrease in the sheet resistance during reduction in O_2 annealing or N_2 and N_2+10%H_2 annealing may be attributed to the increased crystallinity of the varistor [37], which is modified at high

annealing temperatures. The Inter diffusion of Mn and V changes the morphological characteristics of the varistor, thereby affecting the electrical characteristics of the samples. The sheet resistance significantly increases as the annealing temperature increases to more than 400˚C, and this increase is attributed to the agglomeration of the Mn layer [37]. The surface scattering effects of electrons caused by the agglomeration of Mn and the oxidation degree on the surface of Mnvaristor increase, leading to a considerable increase in sheet resistance. The sheet resistance of the varistors annealed in an O_2 atmosphere increases remarkably as annealing temperatures increase. The O_2 chemisorbed easily acts as an acceptor on the surface of the varistor and accordingly decreases the electron concentration. Tansley and Neely [17] reported that the existence of ionized adsorbates on the surfaces of crystallines can increase the height of inter crystalline barriers, thereby minimizing the effective carrier mobilities and conductivities. Another possibility is that Mn has a high diffusion coefficient, and it can migrate rapidly into ZnO varistors during annealing treatment [4]. The diffusion of Mn and V significantly changes the properties of varistors. Mn efficiently decreases mobility and conductivity once it diffuses into the sample because Mn is a deep acceptor in ZnO [38].

Annealing temperature (˚C)	Sheet resistance in Ω/sq in different annealing atmosphere		
	O_2	N_2	N_2+10%H_2
As-grown	12	12	12
200	68.2	9.7	9.2
400	233.1	10.6	11.5
600	610	83.3	110
800	1720	142	152

Table 2: The sheet resistance of ZnO nanoparticles-V_2O_5-Mn_2O_3 varistors annealed under different atmosphere at various temperatures.

Conclusion

ZnO nanoparticle-V_2O_5-Mn_2O_3varistors were prepared through conventional ceramic processing, and the effects of annealing in different atmospheres and at various temperatures on their structural and electrical properties were investigated. sZnO-V_2O_5-Mn_2O_3varistors made from ZnO nanoparticles and annealed in an oxygen atmosphere exhibit optimal performance, good quality, and superior electrical behavior compared with those of other varistors treated under other conditions. The electrical resistivity of the varistors is effectively minimized by thermal annealing in a reducing atmosphere, such as N_2 and N_2+10%H_2, possibly because the passivation of zinc ions and grain boundaries by hydrogen atoms causes an increase in mobility and carrier concentration. However, thermal treatment at temperatures lower than 400˚C is less efficient than that of other temperatures. The lowest resistivity of the varistor is obtained by annealing at 200˚C in N_2+10%H_2 atmosphere and 9.2 Ω/sq sheet resistance, which further increases as annealing temperature increases. This result indicates that the non-ohmic behavior of varistors physically originates from oxygen on grain surfaces adsorbed by intrinsic defects.

References

1. Takada M, Yoshikado S (2010) Effect of thermal annealing on electrical degradation characteristics of Sb-Bi-Mn-Co-added ZnO varistors. Journal of the European Ceramic Society 30: 531-538.
2. Carlson W, Gupta T (1982) Improved varistor nonlinearity via donor impurity doping. Journal of Applied Physics 53: 5746-5753.
3. Lee YS, Liao KS, Tseng TY (1996) Microstructure and crystal phases of praseodymium oxides in zinc oxide varistor ceramics. Journal of The American Ceramic Society 79: 2379-2384.
4. Gattow G, Schroder H (1962) Die Kristallsttrukerder hochtemperature-modikationvon Wismut(III)-oxid (δ-Bi_2O_3). Z. Anorg Allg Chem Band 318: 176.
5. Hng H, Chan P (2004) Microstructure and current-voltage characteristics of ZnO-V_2O_5-MnO_2 varistor system. Ceramics International 30: 1647-1653.
6. Pfeiffer H, Knowles KM (2004) Effects of vanadium and manganese concentrations on the composition, structure and electrical properties of ZnO-rich MnO_2-V_2O_5-ZnO varistors. Journal of the European Ceramic Society 24: 1199-1203.
7. Han J, Senos A, Mantas P (2002) Deep donors in polycrystalline Mn-doped ZnO. Materials Chemistry and Physics 75: 117-120.
8. Kutty TN, Ezhilvalavan S (1995) Influence of alkali ions in enhancing the nonlinearity of ZnO-Bi_2O_3-Co_3O_4 varistor ceramics. Japanese Journal of Applied Physics Part 1 Regular Papers Short Notes and Review Papers 34: 6125-6132.
9. Igasaki Y, Saito H (1991) The effects of zinc diffusion on the electrical and optical properties of ZnO: Al films prepared by r.f. reactive sputtering. Thin Solid Films 199: 223-230.
10. Lu FH, Chen HY (1999) XPS analyses of TiN films on Cu substrates after annealing in the controlled atmosphere. Thin Solid Films 355: 374-379.
11. Studenikin S, Cocivera M, Kellner W, Pascher H (2000) Band-edge photoluminescence in polycrystalline ZnO films at 1.7. Journal of Luminescence 91: 223-232.
12. Zhang D, Brodie D (1994) Effects of annealing ZnO films prepared by ion-beam-assisted reactive deposition. Thin Solid Films 238: 95-100.
13. Szklarski Z, Zakrzewska K, Rękas M (1989) Thin oxide films as gas sensors. Thin Solid Films 174: 269-275.
14. Advani G, Jordan A (1980) Thin films of SnO_2 as solid state gas sensors. Journal of Electronic Materials 9: 29-49.
15. Selim F, Gupta TK, Hower PL, Carlson WG (1980) Low voltage ZnO varistor: Device process and defect model. Journal of Applied Physics 51: 765-768.
16. Putnis A (1195) An introduction to mineral sciences. Cambridge University Press.
17. Tansley T, Neely D (1984) Adsorption, desorption and conductivity of sputtered zinc oxide thin films. Thin Solid Films 121: 95-107.

18. Sagalowicz L, Fox GR (1999) Planar defects in ZnO thin films deposited on optical fibers and flat substrates. Journal of Materials Research 14: 1876-1885.

19. Sanon G, Rup R, Mansingh A (1989) Growth and characterization of tin oxide films prepared by chemical vapour deposition. Thin Solid Films 190: 287-301.

20. Schuler T, Aegerter MA (1999) Optical, electrical and structural properties of sol gel ZnO: Al coatings. Thin Solid Films 351: 125-131.

21. Lin Y, Xie J, Wang H, Li Y, Chavez C, et al. (2005) Green luminescent zinc oxide films prepared by polymer-assisted deposition with rapid thermal process. Thin Solid Films 492: 101-104.

22. Fang Z, Yan ZJ, Tan YS, Liu XQ, Wang YY (2005) Influence of post-annealing treatment on the structure properties of ZnO films. Applied Surface Science 241: 303-308.

23. Liu Y, Tung S, Hsieh J (2006) Influence of annealing on optical properties and surface structure of ZnO thin films. Journal of Crystal Growth 287: 105-111.

24. Tigau N, Ciupina V, Prodan G (2006) Structural, optical and electrical properties of Sb_2O_3 thin films with different thickness. Journal of Optoelectronics and Advanced Materials 8: p. 37.

25. Makarov V, Trontelj M (1194) Novel varistor material based on tungsten oxide. Journal of Materials Science Letters 13: 937-939.

26. Sonder E, Austin M, Kinser D (1983) Effect of oxidizing and reducing atmospheres at elevated temperatures on the electrical properties of zinc oxide varistors. Journal of Applied Physics 54: 3566-3572.

27. Santos MRC, Bueno PR, Longo E, Verela JA (2001) Effect of oxidizing and reducing atmospheres on the electrical properties of dense SnO_2-based varistors. Journal of the European Ceramic Society 21: 161-167.

28. Bueno P, Leite ER, Oliveira MM, Orlandi MO, Longo E (2001) Role of oxygen at the grain boundary of metal oxide varistors: A potential barrier formation mechanism. Applied Physics Letters 79: 48-50.

29. Zielinski E, Vinci R, Bravman J (1994) Effects of barrier layer and annealing on abnormal grain growth in copper thin films. Journal of Applied Physics 76: 4516-4523.

30. Kim ED, Oh MH, Kim CH (1986) Effects of annealing on the grain boundary potential barrier of ZnO varistor. Journal of Materials Science 21: 3491-3496.

31. Verges M, West A (1997) Impedance and modulus spectroscopy of ZnO varistors. Journal of Electroceramics 1: 125-130.

32. Smith A, Baumard JF, Abélard P (1989) ac impedance measurements and V□I characteristics for Co□, Mn□, or Bi□doped ZnO. Journal of Applied Physics 65: 5119-5125.

33. Santos MRC, Bueno PR, Longo E, Verela JA (2001) Effect of oxidizing and reducing atmospheres on the electrical properties of dense SnO_2-based varistors. Journal of the European Ceramic Society 21: 61-167.

34. Yim K, Kim H, Lee C (2013) Effects of annealing on structure, resistivity and transmittance of Ga doped ZnO films. Materials Science and Technology 23:108- 112.

35. Takahashi Y, Kanamori M, Kondoh A, Minoura H, Ohya Y (1994) Photoconductivity of ultrathin zinc oxide films. Japanese Journal of Applied Physics 33: 6611-6615.

36. Look DC, Jones RL, Sizelove JR, Garces NY, Giles NC, et al. (2003) The path to ZnO devices: donor and acceptor dynamics. Physica Status Solidi (a) 195: 171-177.

37. Choi K, Kim JY, Lee Ys, Kim HJ (1999) ITO/Ag/ITO multilayer films for the application of a very low resistance transparent electrode. Thin Solid Films 341: 152-155.

38. Dean P, Robbins DJ, Bishop SG, Savage JA, Porteous P (1981) The optical properties of copper in zinc oxide. Journal of Physics C: Solid State Physics 14: 2847.